Journal of Physics: Conference Series

A data-driven approach for fault diagnosis of drivetrain system in a spar-type floating wind turbine based on the multi-point acceleration measurements

A data-driven approach for fault diagnosis of drivetrain system in a spar-type floating wind turbine based on the multi-point acceleration measurements

Ali Dibaj and Amir R. Nejad and Zhen Gao
Department of Marine Technology, Norwegian University of Science and Technology (NTNU)
E-mail: ali.dibaj@ntnu.no

Abstract. This paper deals with the condition monitoring of a floating wind turbine drivetrain using multi-point acceleration measurements. Single sensor data obtained from drivetrain system may provide insufficient information about the health condition due to the complicated structure and applied loading on this system. As a result, multi-point measurements are required to be employed for reliable fault diagnosis. The shared information between the multi-point measurements can be used for identifying the system's condition. In this study, the fault diagnosis of the floating wind turbine drivetrain system is performed using a data-driven approach. Fault cases are considered in bearings most likely to damage. A combined principal component analysis (PCA) and deep convolutional neural network (CNN) is proposed to extract common and fault-related information between the measurements on the one hand and to classify different health conditions of the drivetrain on the other. It will be demonstrated that PCA-based information provides more satisfactory fault diagnosis results than individual sensor data. The method is numerically validated using the acceleration responses obtained from a 5-MW reference drivetrain model installed on a spar-type floating wind turbine.

1. Introduction

Operation & Maintenance (O&M) costs of offshore wind turbines (WT) are significantly higher than those of onshore WTs [1]. Hence, higher reliable solutions for offshore development is needed than onshore designs. Experiences with the WT's components show that defects in the drivetrain components contribute significantly to the downtime and non-availability of the WT. As a result, employing optimal maintenance strategies on floating WTs, particularly drivetrain components, is crucial. Since the changes caused by system defects appear quickly in vibration signals, vibration-based condition monitoring (often measured as root mean square (RMS) of velocity or acceleration) is a standard method for drivetrain fault diagnosis [2]. Regarding the vibration-based fault diagnosis of drivetrains, Peeters et al. [3] employed cepstrum editing procedure for separating rolling element bearing fault signal from other signals coming from drivetrain elements like gears or shaft. Koukoura et al. [4] proposed a parallel multi-step vibration processing pipelines for planetary stage fault detection in wind turbine drivetrain. Sawalhi et al. [5] analyzed wind turbine drivetrain vibration data provided by the National Renewable Energy Laboratory under a round robin scheme to diagnose bearing and gear faults. However, due to the multi-component structure and multi-source vibration of the drivetrain system, the information obtained from a single sensor is usually limited, and several sensors are needed to be

mounted in various parts of the drivetrain system. A multiple-sensor configuration can provide more comprehensive information on the system's operational state. Nonetheless, using all multi-sensor collected data for condition monitoring, irrelevant information is collected during data acquisition. Therefore, a pre-processing approach should be embedded in the fault diagnosis process in order to get dimension-reduced and fault-related data from raw measurements.

In general, as a fault occurs in the system, the correlations between the multi-point measurements change [6, 7]. By using correlated information between the measurements and fusing them, one can decide about the system's condition. Useful fault-related features can be obtained by capturing the correlated information between the multi-point measurements. Bai et al. [7] studied fault diagnosis of rotor equipment based on multi-sensor correlation analysis and deep learing. A fault diagnosis method has been proposed by Xiong et al. [8] for rotating machinery based on fusing the dimensionless indices and Pearson correlation coefficient. Xin et al. [9] used feature-fusion covariance matrix using multi-sensor data for gearbox fault diagnosis. However, studies on multiple sensor-based fault diagnosis for floating WTs drivetrain systems are limited.

Fault diagnosis of the drivetrain system is performed in this study using shared information from multi-point measurements. The principal component analysis (PCA) method is applied to multi-point raw vibration data to reduce the dimension of the original data and the computational burden while retaining the most possible information. After dimension reduction, the data is fed into a deep convolutional neural network (CNN) for classification and fault-pattern recognition. It will be shown that existing faults in the drivetrain are better diagnosed using information of multiple measurements rather than information obtained from the individual ones.

The 5-MW reference gearbox [10] model is used for numerical validation in this research. simulations are carried out at rated wind speed. This reference gearbox model is installed on a spar-type floating wind turbine. Fault cases are considered in the main bearing, high and intermediate-speed shaft bearings, and planet bearing. These fault cases are most likely locations of the failure based on the previous studies. Changes in the bearing stiffness matrix values in either the radial or axial directions are used to model faults [10, 11, 12]. To include the most failure-related information, acceleration responses are chosen from the parts closest to these faulty bearings. These responses are obtained from the main, low, intermediate, and high-speed shafts.

2. Drivetrain model and methodology

This study uses a 5-MW reference gearbox [10] utilizing commercial SIMPACK software [13], installed on the floating OC3 Hywind spar structure [14, 15]. This WT is a 3-blade upwind turbine with a rated wind speed of 11.4 rpm. The gearbox includes three stages, two planetary and one parallel stage gears. The gearbox was developed with a 4-point support with 2 main bearings to limit entering the non-torque loads to the gearbox. More information about this spar structure and gearbox model can be found in Nejad et al. [16, 10].

The de-coupled analysis approach is employed in order to obtain the vibration responses of the drivetrain model [2] and use them for further procedures. In the de-coupled approach, global and local analyses are separately performed. For global analysis, simulations are done with small sampling frequencies. Because the external excitations - including wave and wind - are in the low-frequency range, often less than 2 Hz. While, for the local analysis, simulations are performed with high sampling frequencies to capture internal excitations - gear mesh frequencies, for example - that are usually within the high-frequency ranges. The overall procedure of the de-coupled analysis approach, as well as the detailed model of the 5-MW reference gearbox and the applied external loads on this model, are shown in Figure 1. More information about global analysis and the parameters used in this analysis can be found in Nejad et al. [2].

As mentioned, internal simulations of the drivetrain system are performed at a high sampling

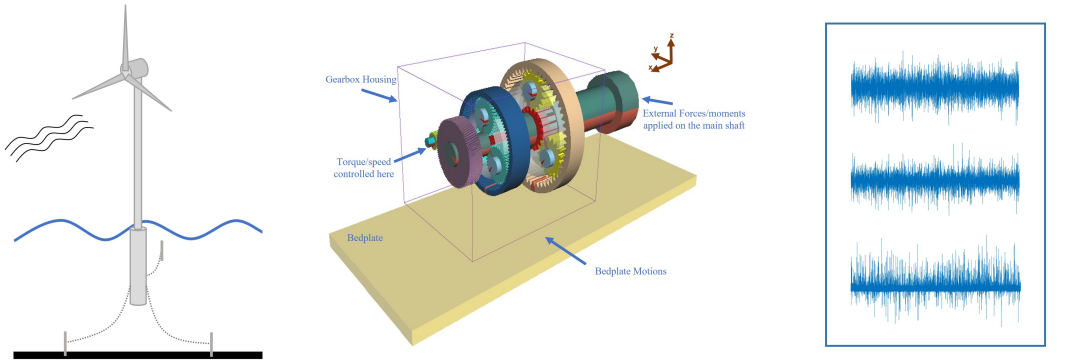

Figure 1. Drivetrain de-coupled analysis method

frequency (200 Hz in this study) to capture all possible internal excitations. For each load case or health condition of the drivetrain, a 3800-second simulation is conducted at rated wind speed. The first 200 seconds are removed during post-processing to prevent temporary start-up effects. In this study, the data analyzed are acceleration measurements obtained from the main, low, intermediate, and high-speed shafts. Fig. 2 shows the location of the measurements. The reason for selecting these locations for investigation in this study is the proximity to the faulty bearings. Changes in system behavior due to defects in bearings can be more clearly identified from these vibration responses.

2.1. Fault cases and fault modeling

Gearbox degradation in wind turbines, as stated by Musial et al. [17], mostly begins with the bearings. Hence, fault cases in a set of bearings are considered in the case study gearbox [10] used in this paper. These bearings are chosen based on the vulnerability map proposed by Nejad et al. [10] and their failure probability. Faults are modeled by change in the stiffness values of the bearings. This approach of bearing fault modeling has been done in some research studies, for example Nejad et al. [2]. Figure 2 and Table 1 show the fault cases considered in this study. The original stiffness values and the reduced values corresponding to degraded bearings in each load case are also given in Table 1.

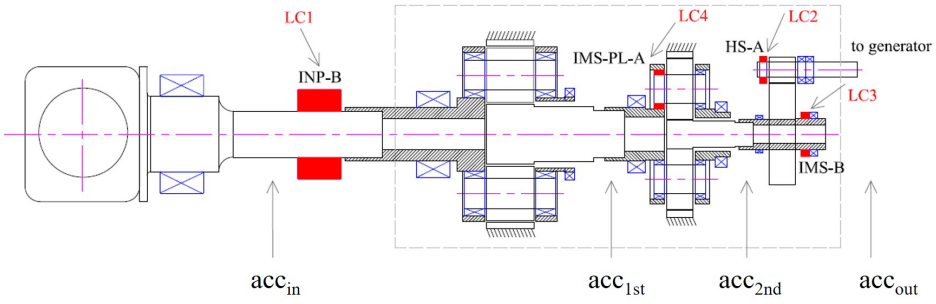

Figure 2. Fault cases and acceleration measurement locations [10]

Table 1. Considered fault cases and corresponding bearing stiffness values

Fault case	Description	Original stiffness value (Healthy) (N/m)	Reduced stiffness value (N/m)
LC0	Reference case, healthy	-	-
LC1	Damage in axial direction of main bearing (INP-B)	4.06×10^8	4.06×10^7
LC2	Damage in radial direction of the high-speed shaft bearing (HS-A)	8.2×10^8	8.2×10^6
LC3	Damage in radial direction of the intermediate-speed shaft bearing (IMS-B)	5×10^8	5×10^6
LC4	Damage in radial direction of the low-speed shaft bearing (IMS-PL-A)	6.12×10^7	6.12×10^5

3. Fault diagnosis approach

3.1. Principal component analysis (PCA)

PCA is a linear feature extraction method that uses dimension reduction of multivariate data [18]. Using PCA, the input data is represented in a smaller dimension space by a set of orthogonal components known as principal components, with the first principal component containing the highest possible variance of the input data.

For a set of normalized multivariate $n\times m$ input data X, where n is the number of observations and m is the number of dimensions, the PCA procedure is as follows:

(i) Compute the $m \times m$ covariance matrix C.

(ii) Compute the eigenvalues λ and eigenvectors Q of the covariance matrix C:

$$Cq = \lambda q \longrightarrow \begin{cases} \lambda_1 \geq \lambda_2 \geq ... \geq \lambda_m \\ Q_{m\times m} = [q_1, q_2, ..., q_m] \end{cases} \tag{1}$$

where each column of Q represents one eigenvector or principal component coefficients for the corresponding eigenvalue.

(iii) Project original space of input data X onto the principal component space:

$$P = Q^T X \tag{2}$$

Both P and X have the same dimension $n \times m$. P contains the principal component scores. Principal component scores are the representations of original data X in the principal component space. Most of the time, the few first principal components are chosen based on the variance threshold.

In this paper, the dimension m equals the number of measurements that is four. The length of measurement vectors is also equal to the number of observations n. PCA's first principal component scores will be used only to retain the direction from the original space with the highest variance.

3.2. Convolutional neural networks (CNN)

In this study, because of using directly simulation data of different healthy and faulty conditions, it is suitable to apply a machine learning-based approach for fault detection and diagnosis. In this regard, CNN as a deep neural network is employed to classify healthy and faulty conditions without the need for hand-crafted features extracted from raw data. CNN networks consist of two parts, as illustrated in Figure 3: feature extractor and classifier. First, high-level features called feature maps are extracted from the input data using multiple convolution and pooling layer pairs in the feature extractor part. The classifier part, which consists of multiple fully connected layers, then assigns the extracted features to the corresponding correct output [19]. The operation in classifier part is similar to that of a multilayer perceptron (MLP) network. The output layer typically uses the Softmax activation function for multi-class classification. This activation function returns the conditional probability for each class as output. Assuming that there are N classes to classify the data, the probability of output y corresponding to the kth node or class ($O_k \in [0, 1]$) in the output layer with the Softmax function is calculated as follows [20]:

$$O_k = P(y = k|x; W_k, b_k) = Softmax(W_k x + b_k) = \frac{exp(W_k x + b_k)}{\sum_{i=1}^{N} exp(W_i x + b_i)} \tag{3}$$

where $P(.)$ is the conditional probability function, x is the input of output layer and $\sum_{i=1}^{N} O_i = 1$. W_k and b_k are also weight and bias values corresponding to kth node. The output node corresponding to the maximum value of the conditional probability obtained is considered as the input data class.

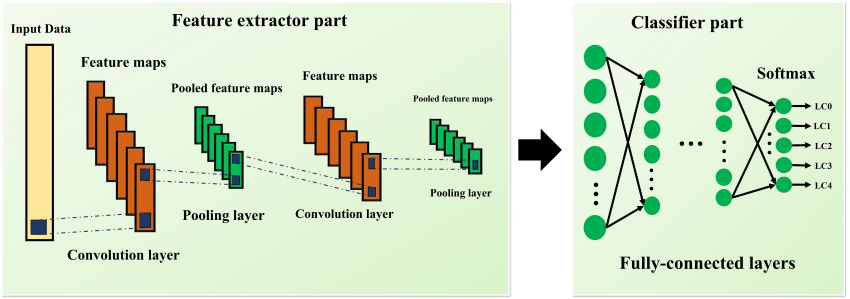

Figure 3. CNN architecture

3.3. Overall proposed procedure - Combining PCA and CNN

In this study, the drivetrain fault diagnosis method is performed in a pattern recognition framework. First, the multi-point acceleration measurements are segmented into shorter-length responses to generate enough data for training and testing the CNN model. PCA is applied to multi-point segmented measurements in the feature extraction step. This applying is done for two reasons: (1) to reduce the computational burden and (2) to obtain shared information between the measurements by retaining the most dominant direction in the original data. The first principal component is used for this purpose. The classification step also includes feeding the PCA-projected responses into the CNN to determine the health condition of the drivetrain system. Figure 4 depicts the steps taken to fault diagnosis in this paper.

4. Results and discussion

For fault diagnosis through the CNN model, we need to have sufficient data for training step. In this regard, we should segment the original responses obtained in each load case. 1-hour

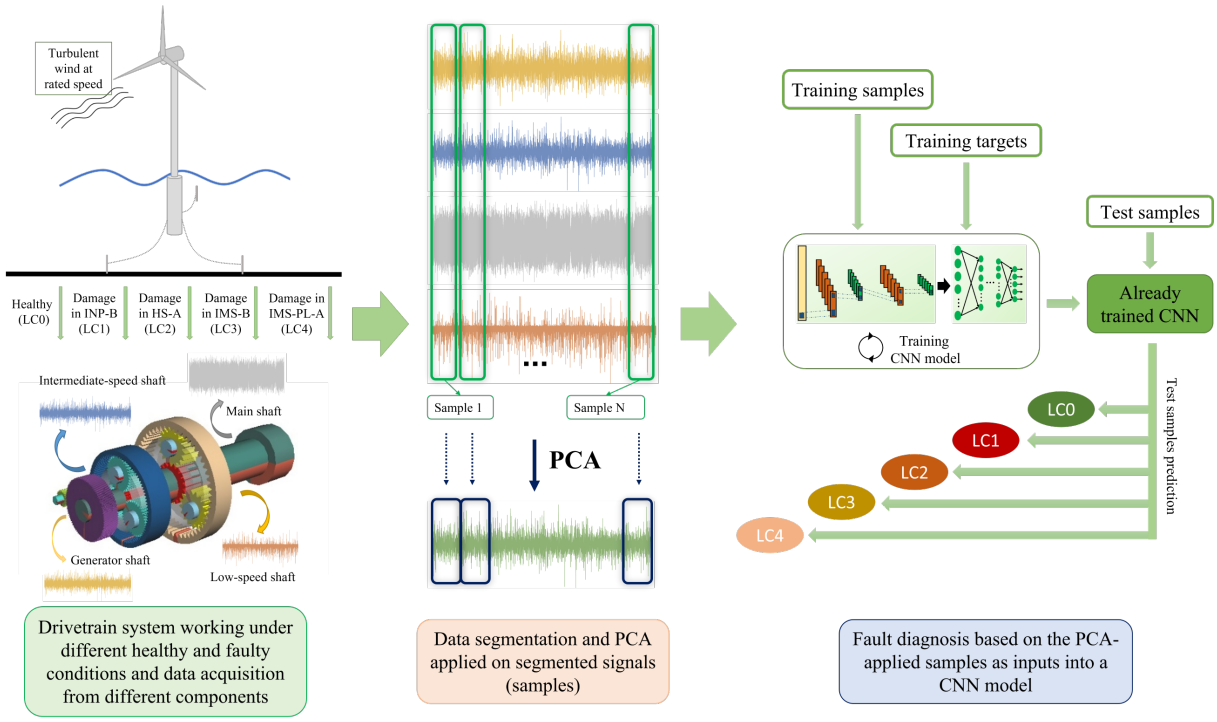

Figure 4. Schematic description of the proposed method for the fault diagnosis of the drivetrain

measurements collected for each load case are segmented into shorter-length signals with 10 seconds length. For each load case, 270 segmented signals are considered (1350 signals in total), each with a length of 2000 sample points. This segmentation should be short enough to contain the required information from the system. On the other hand, segmented signals should be statistically different and have statistical variation.

Multi-point acceleration measurements are collected from the main, low-speed, intermediate-speed and high-speed shafts. The PCA method is employed to extract the possible correlated information between these measurements by reducing the dimensions of the original data. The dimension reduction is performed by reducing four dimensions (number of measurements) to just one dimension by retaining the first principal component. In the classification stage, 1D CNN is implemented to be fed by PCA-projected data. The input length of the CNN model is considered the same as the length of the segmented signals or 2000. The output number of this model is also the same as the number of load cases (fault conditions) which is 5. 75% of the segmented signals or samples are used as training data, and the rest as test data. The results for test data are presented as the classification accuracy for each class, as well as the overall accuracy in Table 2. In addition, the CNN model is trained separately with four individual measurements for comparison. The obtained results can also be found in Table 2. The purpose of this comparison is to see if correlated information obtained through PCA can outperform information obtained from single sensors in fault diagnosis.

As seen from the results of Table 2, when the CNN model is trained with data from the individual sensors, the highest classification accuracy is obtained for the fault condition near that sensor. For example, in the case of trained CNN with only data from acc_{in} (measurements close to the main bearing), test samples for the LC1 (fault in the main bearing) are correctly classified. While the other conditions have poor classification accuracy. This is also true for the trained CNN with only data from acc_{1st}. In this case, all test samples related to the failure in the IMS-PL-A bearing (LC4) are correctly recognized. However, for acc_{2nd}, it is also expected

that the fault in the IMS-B bearing located at the end of the intermediate-speed shaft (LC3) can be correctly classified. But, we see that it is incapable of accurately detecting this condition. There is another bearing next to this faulty bearing (IMS-A). These are taper-type bearings that are usually installed in pairs. The IMS-A bearing impedes additional loads caused by IMS-B failure. As a result, slight vibration occurs from the IMS-B bearing failure, and it cannot be distinguished from the healthy condition. Furthermore, the classification results are more accurate when acceleration data from the high-speed side of the drivetrain is used. Trained CNNs with acc_{2nd} and acc_{out} provide higher classification accuracy than acc_{in} and acc_{2nd}. These results were predictable, as the acceleration measurements are more sensitive to high impact rates. Low-speed side measurements contain less impact energy, due to the damaged bearings, than high-speed side acceleration measurements. The low impact energy results in a high ratio of noise to an abnormal bearing signal [21]. Therefore, measurements of the high-speed side of the drivetrain can provide more fault-related information. These results are also seen in the confusion matrix obtained for each trained CNN model in Figures 5 (a)-(d). As can be seen, all trained models with individual measurements, especially acc_{in} and acc_{1st}, have poor classification accuracy in fault cases located far from the location of the used measurement. This misclassification in fault cases also results in poor detection accuracy for healthy condition. Because non-detectable test samples from each fault case, especially LC3, are incorrectly classified in the healthy class.

Table 2. Fault diagnosis accuracy for test dataset in each class and overall accuracy (CNN model is trained with different inputs)

Input to CNN	LC0 (%)	LC1 (%)	LC2 (%)	LC3 (%)	LC4 (%)	Overall (%)
acc_{in}	21.11	100.00	53.33	24.44	48.89	**49.56**
acc_{1st}	28.89	24.44	21.11	26.67	100.00	**40.22**
acc_{2nd}	65.56	62.22	100.00	50.00	100.00	**75.56**
acc_{out}	73.33	95.56	100.00	61.11	74.44	**80.89**
Proposed method	77.78	97.78	98.89	86.67	91.11	**90.45**

The results for the trained CNN with PCA-based data (proposed method) are also given in Table 2 and Figure 5 (e). As discussed earlier, the first principal component is chosen as the input to the CNN model. This component corresponds to the direction with the maximum variance in the original data space. As a result, this component is just retained to represent all measurements. As can be seen, compared to the results of individual measurements, all fault classes can be classified more accurately (over 90 percent in overall accuracy), and the results are more reliable. However, as illustrated by the confusion matrix in Figure 5, most incorrectly classified samples belong to the LC0 and LC3 classes. As previously stated regarding LC3, fault signatures are masked by the paired bearing. Hence, a few LC3 class test samples (15.6%) and some healthy test samples (11.1%) are misclassified. Also, there are some other incorrectly classified samples in other classes. This misclassification could be related to the performance of CNN model. Changing the CNN training parameters and layer configuration might enhance detection accuracy. However, the purpose of this study was to compare PCA-based results with the fault diagnosis results acquired from individual measurement data. The findings in the current study show that information obtained using PCA from the multi-point acceleration data is more effective in fault diagnosis compared to the individual measurements.

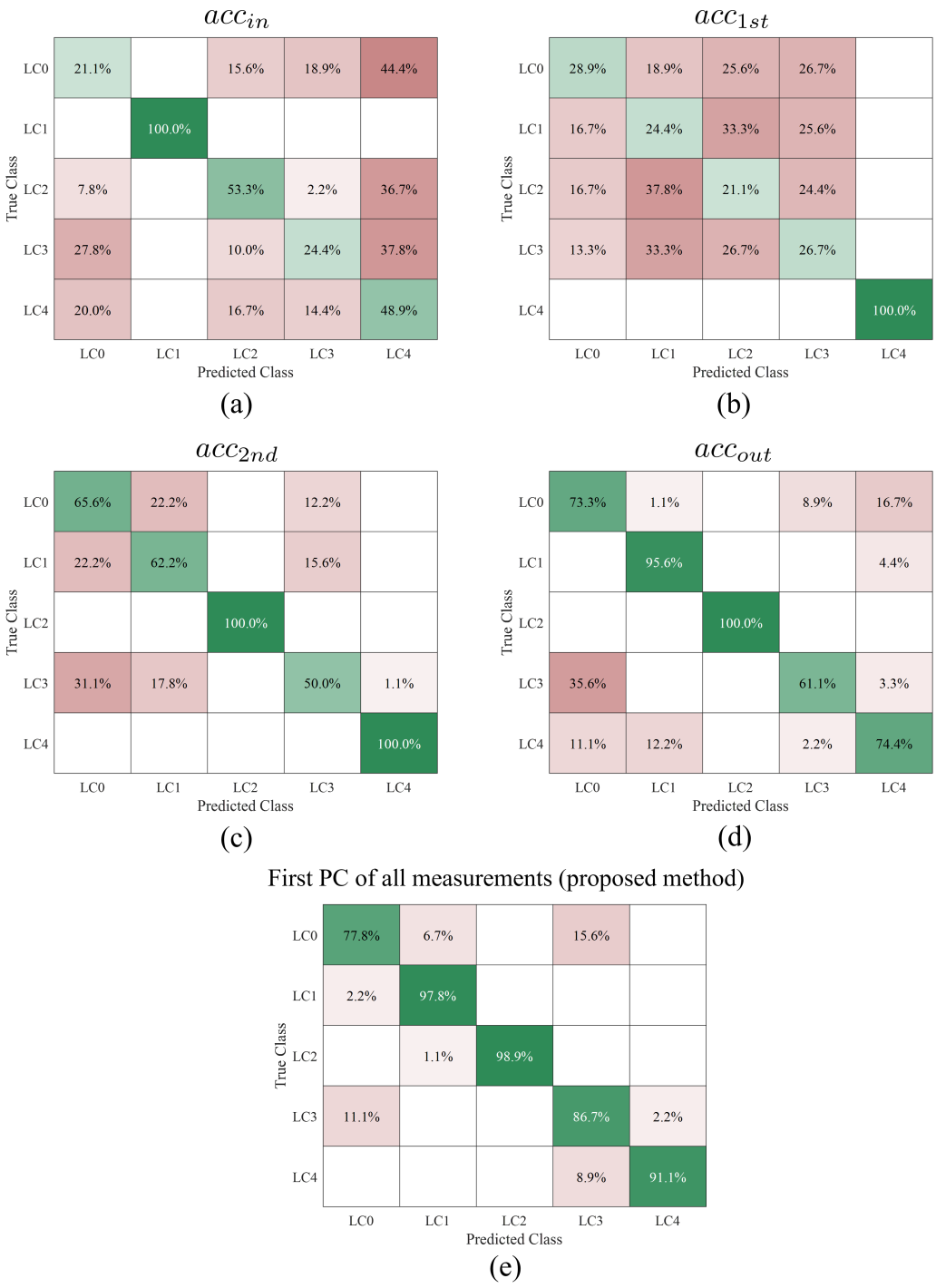

Figure 5. Fault diagnosis results for test dataset in the form of confusion matrix with different inputs for CNN model: (a) acc_{in} (b) acc_{1st} (c) acc_{2nd} (d) acc_{out} (e) First principal component obtained from all measurements

5. Conclusion

In this study, fault diagnosis of the drivetrain system was performed using the multi-point acceleration measurements and a data-driven approach. The case study is a 5-MW drivetrain simulated model installed on a spar-type floating wind turbine. Numerical measured data are

acceleration responses obtained from the main, low-speed, intermediate-speed, and generator shafts. Fault cases were studied on the main bearing (LC1), the generator shaft bearing (LC2), the bearing at the end of the intermediate-speed shaft (LC3), and the low-speed shaft planet bearing (LC4). PCA was employed to reduce the dimension of the multi-point measurements. PCA-projected data were then fed into a deep CNN model to classify the drivetrain's different healthy and faulty conditions. It was shown that the multi-point information obtained through PCA performs better in fault diagnosis than individual measurements. Furthermore, acceleration measurements from the high-speed side of the drivetrain were found to be more accurate in fault diagnosis than measurements from the low-speed side.

For future studies, it will be demonstrated which combinations of acceleration measurements result in higher accuracy for fault diagnosis. This analysis will aid in the sensor optimization problem by getting better condition monitoring measurements. It can be investigated by studying the correlation between the measurements and how their relationship changes when a fault occurs in one of the components. In addition, in this study, the first principal component was only used as condition monitoring data. Although this component has the maximum original data variance, the following components are also likely to contain fault-related information based on their correlation to original data and which direction they include in the original data space. As a result, a study will be done on the required number of principal components representing all the original measurements. A comparative analysis of radial and axial acceleration measurements for fault diagnosis is also of interest for future work.

Acknowledgment
The authors gratefully acknowledge the financial support of the Research Council of Norway through the InteDiag-WTCP project (Project Number 309205).

References

[1] Pablo Hevia-Koch and Henrik Klinge Jacobsen. "Comparing offshore and onshore wind development considering acceptance costs". In: *Energy Policy* 125 (Feb. 2019), pp. 9–19. ISSN: 0301-4215. DOI: 10.1016/J.ENPOL.2018.10.019.

[2] Amir R. Nejad, Peter Fogh Odgaard, and Torgeir Moan. "Conceptual study of a gearbox fault detection method applied on a 5-MW spar-type floating wind turbine". In: *Wind Energy* 21.11 (2018), pp. 1064–1075. ISSN: 10991824. DOI: 10.1002/we.2213.

[3] Cédric Peeters, Patrick Guillaume, and Jan Helsen. "Vibration-based bearing fault detection for operations and maintenance cost reduction in wind energy". In: *Renewable Energy* 116 (2018), pp. 74–87. ISSN: 18790682. DOI: 10.1016/j.renene.2017.01.056.

[4] Sofia Koukoura et al. "Investigating parallel multi-step vibration processing pipelines for planetary stage fault detection in wind turbine drivetrains". In: *Journal of Physics: Conference Series* 1618.2 (2020). ISSN: 17426596. DOI: 10.1088/1742-6596/1618/2/022054.

[5] Nader Sawalhi, Robert B. Randall, and David Forrester. "Separation and enhancement of gear and bearing signals for the diagnosis of wind turbine transmission systems". In: *Wind Energy* 17.5 (May 2014). ISSN: 10954244. DOI: 10.1002/we.1671.

[6] Young Jun Yoo. "Data-driven fault detection process using correlation based clustering". In: *Computers in Industry* 122 (2020). ISSN: 01663615. DOI: 10.1016/j.compind.2020.103279.

[7] Tangbo Bai et al. "Fault Diagnosis Method Research of Mechanical Equipment Based on Sensor Correlation Analysis and Deep Learning". In: *Shock and Vibration* 2020 (2020). ISSN: 10709622. DOI: 10.1155/2020/8898944.

[8] Jianbin Xiong et al. "The Order Statistics Correlation Coefficient and PPMCC Fuse Non-Dimension in Fault Diagnosis of Rotating Petrochemical Unit". In: *IEEE Sensors Journal* 18.11 (2018), pp. 4704–4714. ISSN: 1530437X. DOI: 10.1109/JSEN.2018.2820170.

[9] Xin Li et al. "Multi-sensor gearbox fault diagnosis by using feature-fusion covariance matrix and multi-Riemannian kernel ridge regression". In: *Reliability Engineering and System Safety* 216.August (2021), p. 108018. ISSN: 0951-8320. DOI: 10.1016/j.ress.2021.108018. URL: https://doi.org/10.1016/j.ress.2021.108018.

[10] Amir Rasekhi Nejad et al. "Development of a 5 MW reference gearbox for offshore wind turbines". In: *Wind Energy* (2016). ISSN: 10991824. DOI: 10.1002/we.1884.

[11] Amir Rasekhi Nejad et al. "A prognostic method for fault detection in wind turbine drivetrains". In: *Engineering Failure Analysis* 42 (2014), pp. 324–336. ISSN: 13506307. DOI: 10.1016/j.engfailanal.2014.04.031. URL: http://dx.doi.org/10.1016/j.engfailanal.2014.04.031.

[12] Mahdi Ghane et al. "Condition monitoring of spar-type floating wind turbine drivetrain using statistical fault diagnosis". In: *Wind Energy* 21.7 (2018), pp. 575–589. ISSN: 10991824. DOI: 10.1002/we.2179.

[13] *Simpack MBS Software | Dassault Systèmes*. URL: https://www.3ds.com/products-services/simulia/products/simpack/.

[14] Jm Jonkman et al. "Definition of a 5-MW reference wind turbine for offshore system development". In: *Contract* (2009). ISSN: 01487299.

[15] J Jonkman. "Definition of the Floating System for Phase IV of OC3". In: *Contract* (2010).

[16] Amir Rasekhi Nejad et al. "Stochastic dynamic load effect and fatigue damage analysis of drivetrains in land-based and TLP, spar and semi-submersible floating wind turbines". In: *Marine Structures* 42.7491 (2015), pp. 137–153. ISSN: 09518339. DOI: 10.1016/j.marstruc.2015.03.006. URL: http://dx.doi.org/10.1016/j.marstruc.2015.03.006.

[17] Walt Musial, Sandy Butterfield, and Brian Mcniff. "Improving wind turbine gearbox reliability". In: *European Wind Energy Conference and Exhibition 2007, EWEC 2007*. 2007. ISBN: 9781622764686.

[18] I T Jolliffe. *Principal Component Analysis. Second Edition*. 2002. ISBN: 0387954422. DOI: 10.2307/1270093.

[19] Yann LeCun et al. "Gradient-based learning applied to document recognition". In: *Proceedings of the IEEE* 86.11 (1998). ISSN: 00189219. DOI: 10.1109/5.726791.

[20] Ali Dibaj et al. "A hybrid fine-tuned VMD and CNN scheme for untrained compound fault diagnosis of rotating machinery with unequal-severity faults". In: *Expert Systems with Applications* 167 (Apr. 2021), p. 114094. ISSN: 0957-4174. DOI: 10.1016/J.ESWA.2020.114094.

[21] A. C.C. Tan, Y. H. Kim, and V. Kosse. "Condition monitoring of low-speed bearings - A review". In: *Australian Journal of Mechanical Engineering* 6.1 (2008), pp. 61–68. ISSN: 14484846. DOI: 10.1080/14484846.2008.11464558.